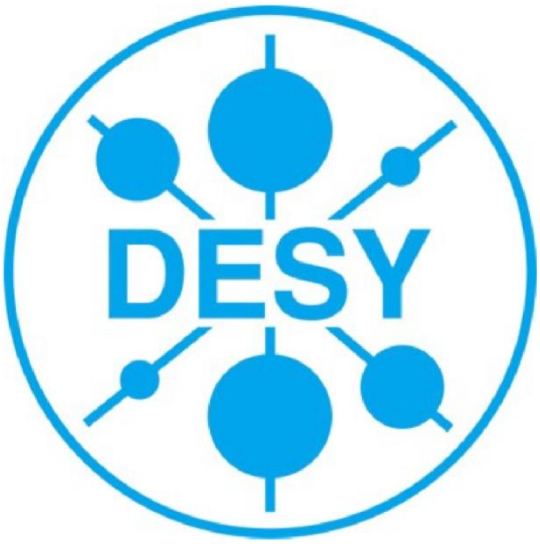

Intensity correlations in spectral domain at PAL-XFEL experiments

Egorov Daniil, Lomonosov Moscow State University, Russia

September 2019

Supervisors:

Khubbutdinov Ruslan

Prof. Dr. Ivan A. Vartanyants

Abstract

We present measurements of second-order intensity correlation functions in the frequency domain performed at the Pohang Accelerator Laboratory X-ray Free Electron Laser (PAL-XFEL, Pohang, Korea) in the saturated regime of its operation. We characterize the temporal coherence properties of hard X-ray pulses, which are very important for the correct interpretation of the experimental data. Intensity correlation measurements in spectral domain gave an estimate of the PAL-XFEL average pulse duration that was determined to be 17 fs. In the Self Amplification Spontaneous Emission regime, the analysis of the intensity distribution provides an estimate for the number of longitudinal modes. We also obtained the coherence time of hard X-ray pulses that was 0.6 fs.

Contents

I. Introduction

X-ray Free Electron Lasers (XFELs) deliver orders of magnitude more brilliance, nearly fully transverse coherent and ultrashort X-ray pulses than previously available at synchrotron storage-ring based sources. These unique properties enable probing complex structural dynamics down to femtosecond time-scales by means of optical-pump X-ray-probe scattering, X-ray photon correlation spectroscopy, and single-pulse coherent diffraction imaging. In this regard, many XFEL experiments, therefore, rely on the coherence properties of the radiation. Coherence properties of X-ray beams can be characterized by the speckle contrast or the visibility of coherent diffraction patterns. Their value range between zero (no coherence) up to unity (full coherence).

Coherence properties of the XFEL radiation differ from that of optical lasers because of the initial electron beam shot-noise that gets amplified during the Self-Amplified Spontaneous Emission (SASE) process. While the beam is expected to be nearly fully transversely coherent, in which the output radiation is dominated by a single spatial mode near SASE saturation, each XFEL pulse carries multiple temporal modes. The energy distribution among these modes varies randomly for subsequent X-ray pulses resulting in intensity fluctuations. Such behavior is strongly coupled to the details of the operational parameters of the accelerator. Therefore, the characterization of the single-shot and average coherence properties of XFEL pulses is essential for these new light sources to realize their full potential.

Intensity interferometry, as introduced by Hanbury Brown and Twiss [1, 2], was a revolutionary experiment at the time. Their measurements, seemingly showing a contradiction between classical and quantum theories of light, led to the development of quantum optics [3]. Since then, HBT interferometry has found applications in many areas of physics. Intensity-intensity correlation measurements in the x-ray energy range were first suggested to solve the phase problem in crystallography [4], further developed conceptually, and finally performed at synchrotron sources [5-7]. The correlation of intensities at two points in space, expressed in terms of the degree of second-order coherence, is particularly well suited for interferometry at FEL sources. The femtosecond pulse duration of the FEL radiation allows the elimination of the necessity for a correlator device to perform

coincidence measurements. In comparison with Young's interferometry, where the double-pinhole separation must be changed to measure coherence between different spatial positions, the HBT approach with a pixelated detector allows one to measure the correlation function at a set of distances simultaneously. As soon as intensity and not amplitude correlations are measured in an HBT experiment, this method is not sensitive to phase fluctuations, which can significantly affect Young's or Michelson interferometry. Importantly, the HBT experiment provides the possibility of high-order statistical analysis of FEL radiation properties.

II. Theory

a) Second-order intensity correlation function.

The core idea of the HBT experiment is to determine second-order intensity correlation function by measuring intensity in two separated points

$$g^{(2)}(t_1, t_2) = \frac{\langle I(t_1) \cdot I(t_2) \rangle}{\langle I(t_1) \rangle \langle I(t_2) \rangle}. \qquad (2.1)$$

In Eq. (2.1), $I(t_1), I(t_2)$ are the intensities of the wave in corresponding points of time and the averaging denoted by brackets $\langle \dots \rangle$ is performed over a large ensemble of different realizations of the wave field or different pulses in the case of XFEL radiation.

The chaotic sources with Gaussian statistics may be described by following intensity correlation function

$$g^{(2)}(t_1, t_2) = 1 + \xi_2(D_\omega)|\mu(t_1, t_2)|^2. \qquad (2.2)$$

Here $\xi_2(D_\omega)$ is the contrast function which in the case of chaotic sources depends strongly on the radiation frequency bandwidth (D_ω). The complex degree of coherence $\mu(t_1, t_2)$ is defined as $\mu(t_1, t_2) = J(t_1, t_2)/\sqrt{\langle I(t_1) \rangle}\sqrt{\langle I(t_2) \rangle}$, where $J(t_1, t_2)$ is the mutual coherence function (MCF) determined at the detector position.

The coherence time of the wave field can be estimated as

$$\tau_c = 2\pi/D_\omega. \qquad (2.3)$$

b) Determination of the pulse duration from the intensity interferometry.

The contrast function $\xi_2(D_\omega)$ introduced in Eq. (2.2) can be determined from the values of the intensity correlation function along the main diagonal $g^{(2)}(t, t)$ Fig. (4). Assuming the Gaussian Shell-model pulsed source, the contrast function $\xi_2(D_\omega)$ can be expressed as [8]

$$\xi_2(D_\omega) = \frac{1}{\sqrt{1+4(T_{rms}D_\omega)^2}}, \qquad (2.4)$$

where T_{rms} is an effective pulse duration. Inversion of equation (2.4) gives, for the FWHM of the pulse duration,

$$T = \frac{2.355}{2D_\omega}\sqrt{\frac{1}{[(D_\omega)]^2} - 1}. \qquad (2.5)$$

c) Intensity distribution for chaotic sources. In case of chaotic sources, intensity distribution obeys Gaussian statistics and the probability density function $p(I)$ follows a Gamma distribution

$$p(I) = \frac{M^M}{\Gamma(M)} \left(\frac{I}{\langle I \rangle}\right)^{M-1} \frac{1}{\langle I \rangle} exp\left(-M \frac{I}{\langle I \rangle}\right), \qquad (2.6)$$

where $\langle I \rangle$ is an average intensity of the pulse, $\Gamma(M)$ is gamma function of argument $M$and

$$M^{-1} = \sigma^2. \qquad (2.7)$$

Here σ^2 is the normalized dispersion of the intensity distribution is calculated as follows:

$$\sigma^2 = \frac{\langle (I - \langle I \rangle)^2 \rangle}{\langle I \rangle^2}. \qquad (2.8)$$

In the Eqs. (2.6, 2.7) parameter M can be interpreted as the average number of "degree of freedom" or "modes" in a radiation pulse [9, 10].

III. Results

Measurements were performed at the Pohang Accelerator Laboratory X-ray Free Electron Laser (PAL-XFEL, Pohang, Korea). Using full-range spectrometer (1800x300 pxl) there were recorded 2494 shots on the first day and 1255 shots on the second day. An example of the single multimode pulse is shown in Fig. (1). From every shot, there were selected peaks with intensity threshold 5% of the maximum possible intensity. The mean value of the number of these peaks or "modes" was 36 ± 8 for the first day and 38 ± 12 for the second day of measurements.

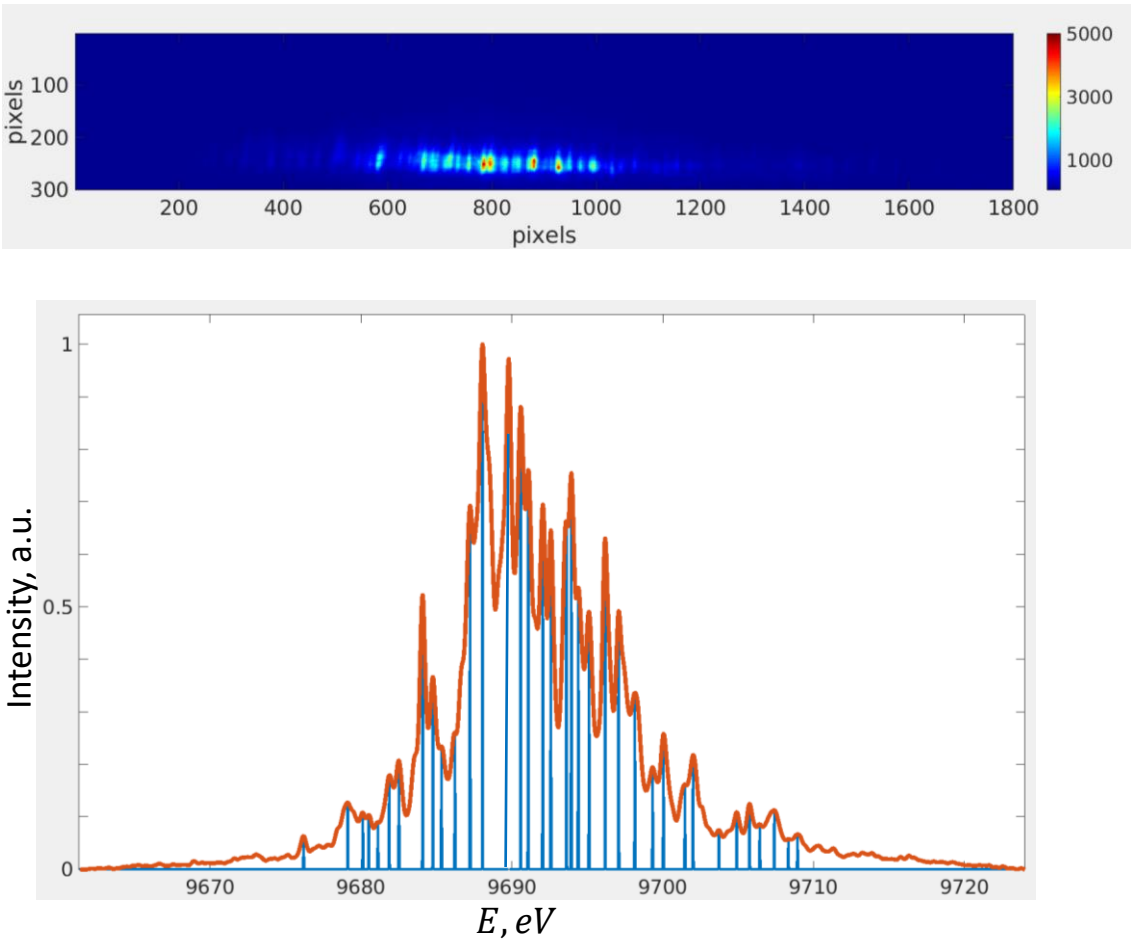

Fig. 1 Example of SASE spectra for pulse recorded using the full-range spectrometer and converted in frequency domain (red line). Blue vertical lines show peaks selected to calculate the number of modes.

For these two data sets, we first analyzed averaged intensity distribution converted in energy domain (see Fig. 2). Using fit by Gaussian function we obtained a mean value of resonance energy of $9691.5 \pm 6.6\text{eV}$ and $9699.5 \pm 6.9\text{eV}$ for the first and second days of

measurements, respectively. As a result we see an energy drift of 8 eV between two days of measurements.

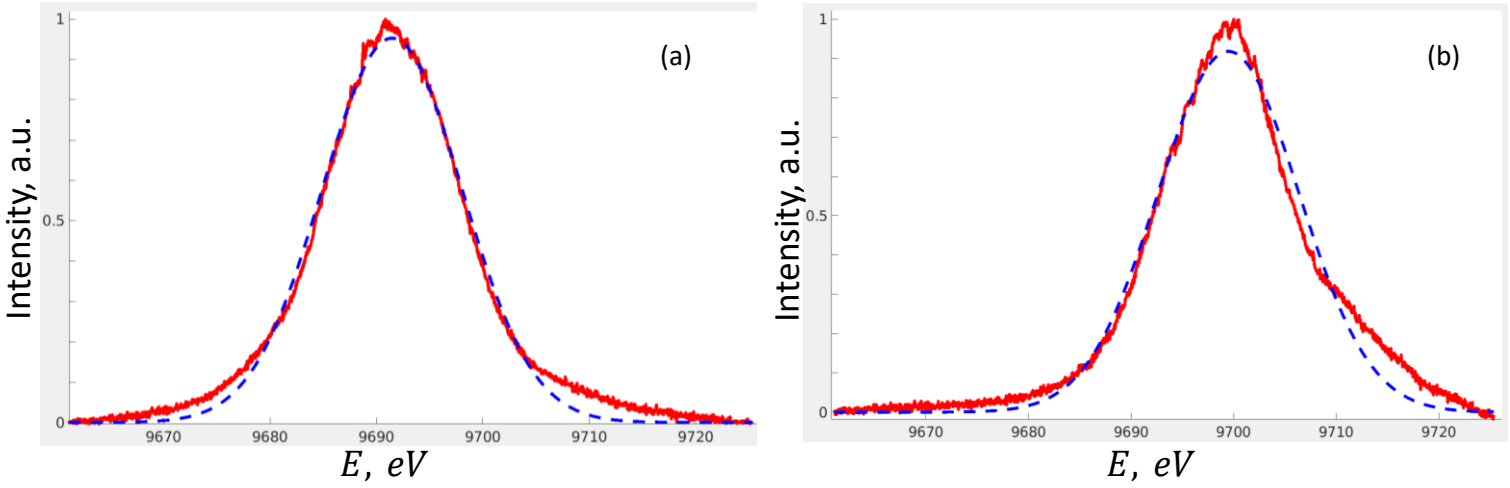

Fig. 2 Averaged intensity distributions for the 1-st (a) and 2-nd (b) days of measurements. Red line is the experimental data, blue dashed line is the Gaussian fit.

Using relation (2.3) we also estimated the coherence time of the pink beam, which was $\tau_c = 0.62$ fs and $\tau_c = 0.63$ fs for the first and second days of measurements, respectively.

The second-order intensity correlation function in spectral domain $g^{(2)}(\omega_1, \omega_2)$ is shown in Fig. (3).

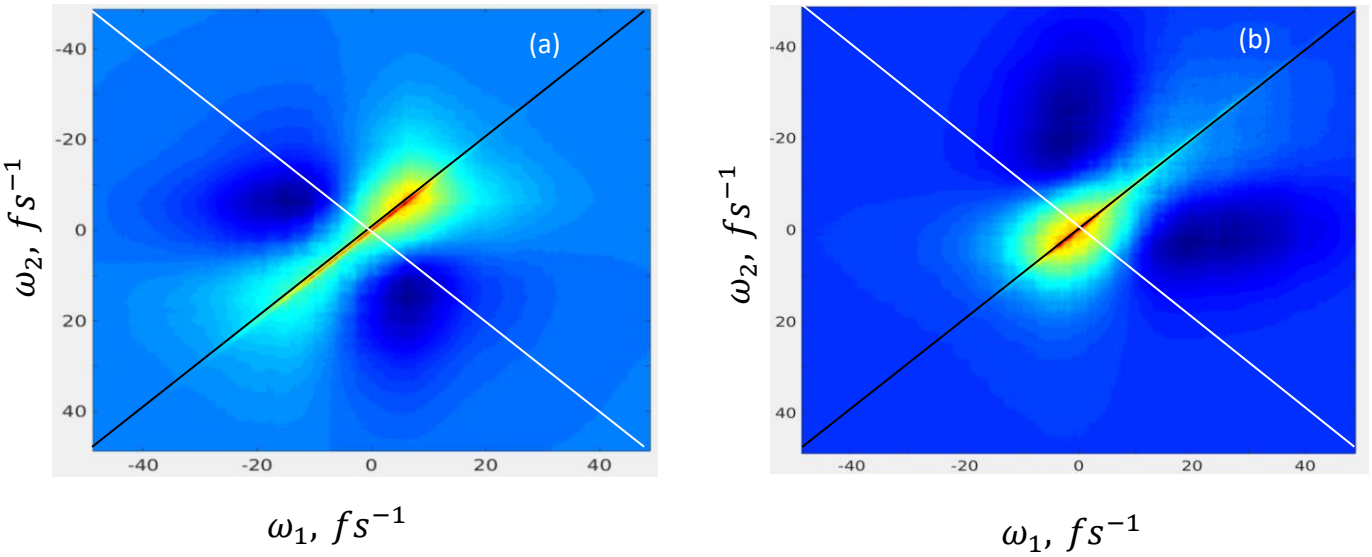

Fig. 3 Intensity correlation functions for the 1-st (a) and 2-nd (b) days of measurements.

Fig. 4 represents the correlation function $g^{(2)}(\Delta\omega)$ taken along the white diagonal. Here we can see some features: function $g^{(2)}(\Delta\omega)$ drops below unity and appears an additional

broad peak. We assume that these features may occur due to the positional and energy jitter.

A Gaussian fit $g^2(\Delta\omega) = 1 + G(\Delta\omega_1,\sigma_1) + G(\Delta\omega_2,\sigma_2)$ [where $G(\Delta\omega,\sigma) = \frac{e^{-(\Delta\omega)^2/2\sigma^2}}{\sigma\sqrt{2\pi}}$] was used to determine the pulse duration from the measurements of second-order correlation function $g^{(2)}(\Delta\omega)$ (Fig. 4). The narrow peaks provided us with r.m.s. values in spectral domain $\sigma_\omega^{(n,1)} = 0.312\ fs^{-1}$ and $\sigma_\omega^{(n,2)} = 0.316\ fs^{-1}$ for the first and second days. From here we obtained an averaged pulse duration of 8.54 fs and 8.45 fs (FWHM) for the first and second days of measurements, respectively. For the broad peaks we obtained the r.m.s. values in spectral domain $\sigma_\omega^{(b,1)} = 4.860\ fs^{-1}$ and $\sigma_\omega^{(b,2)} = 7.594\ fs^{-1}$ for the first and second days.

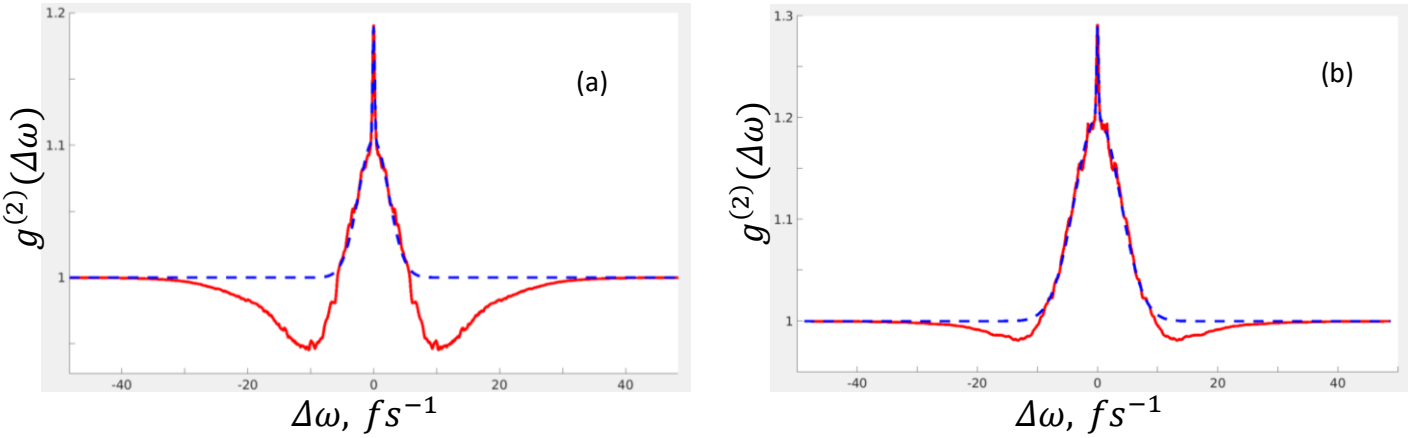

Fig. 4 White diagonal cross sections of intensity correlation functions for the 1-st (a) and 2-nd (b) days of measurements (red line). Blue dashed line is the double Gaussian fit to the $g^{(2)}$ correlation function.

The results of our calculations also indicate that the statistical properties of the beam are not spatially uniform. This is well visualized by the inspection of the beam fluctuations $g^{(2)}(\omega,\omega) = \langle I^2(\omega)\rangle/\langle I(\omega)\rangle^2$ along the beam profile [see Fig. 5].

Typical histograms of pulse intensities for different days of measurements are shown in Fig. 6. Using the technique described in section II (c) [Eq. (2.6-2.8)] we obtained a number of longitudinal modes M that were 11 for the first day of measurements and 20 for the second day.

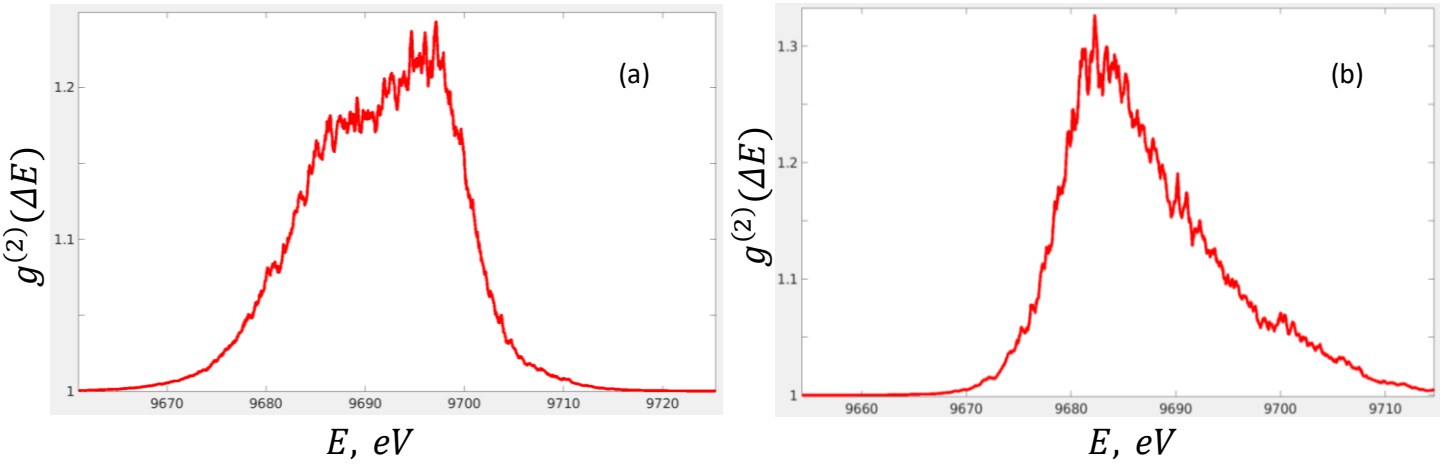

Fig. 5 Dark diagonal cross sections of intensity correlation functions for the 1-st (a) and 2-nd (b) days of measurements.

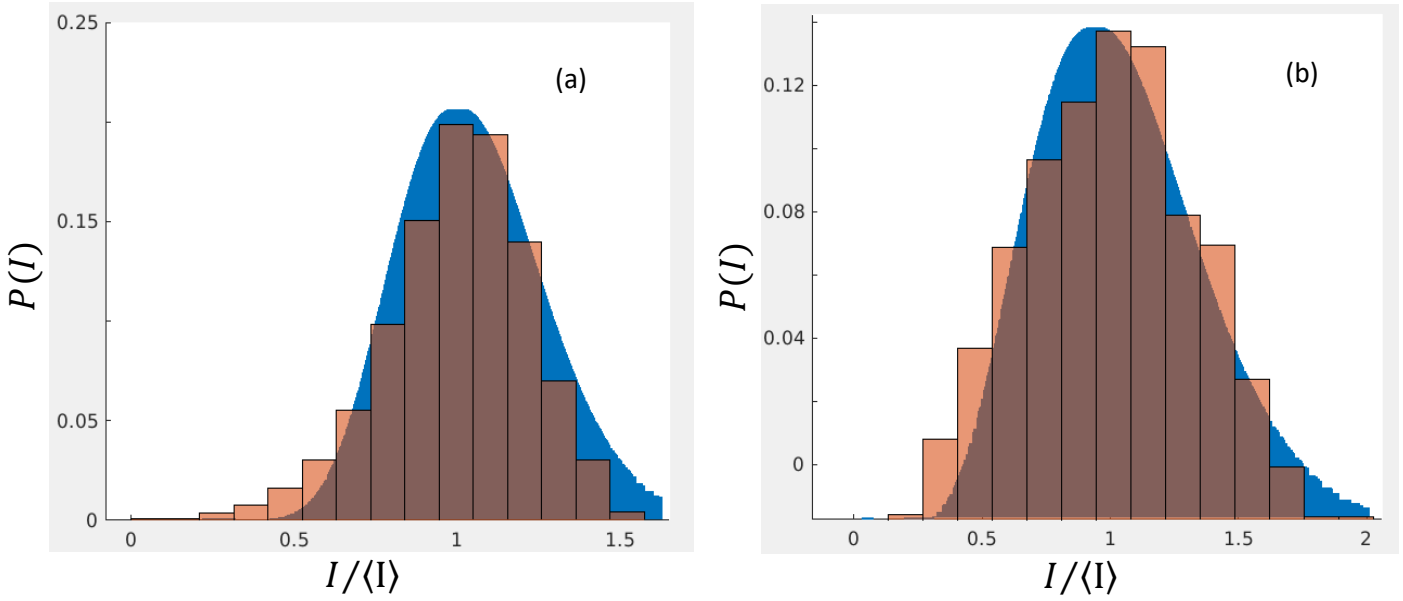

Fig. 6 Histograms of the probability density distribution, $p(I)$, of the total radiation intensity I detected during the time T, for the 1-st (a) and 2-nd (b) days of measurements. The measurement parameter M is connected by relation (2.7). $\langle I\rangle$ denotes the average energy. The blue area represents a fit by gamma function (2.6).

IV. Conclusion

In summary, it was demonstrated how the HBT method can be applied to the analysis of the coherence properties of new generation x-rays radiation sources. It was shown how such essential values as coherence time (τ_c), number of longitudinal modes (M) and pulse duration (T) can be obtained from the HBT analysis and can be used for the understanding of coherence-based experiments. For two data sets, we received the following values: $\tau_c = 0.62$ fs and 0.63 fs; $M = 36 \pm 8$ and 38 ± 12; $T = 8.54$ fs and 8.45 fs for the first and second days of measurements, respectively. We assume that features in the behavior of second-order correlation function $g^{(2)}(\Delta\omega)$ such as the appearance of an additional broad peak and drop of this function below unity appear due to the positional and energy jitter.

V. References

[1] R. Hanbury Brown and R. Q. Twiss, *Nature* (London) **177**, 27 (1956).

[2] R. Hanbury Brown and R. Q. Twiss, *Nature* (London) **178**, 1046 (1956).

[3] R. J. Glauber, *Phys. Rev*. **130**, 2529 (1963).

[4] M. L. Goldberger, H. W. Lewis, and K. M. Watson, *Phys. Rev*. **142**, 25 (1966).

[5] E. Gluskin, E. E. Alp, I. McNulty, W. Sturhahn, and J. Sutter, *J. Synchrotron Radiat*. **6**, 1065 (1999).

[6] M. Yabashi, K. Tamasaku, and T. Ishikawa, *Phys. Rev. Lett*. **88**, 244801 (2002).

[7] A. Singer, U. Lorenz, A. Marras, A. Klyuev, J. Becker, K. Schlage, P. Skopintsev, O. Gorobtsov, A. Shabalin, H.-C. Wille et al., *Phys. Rev. Lett*. **113**, 064801 (2014).

[8] A. Singer. *Coherence properties of third and fourth generation x-ray sources. Theory and experiment*. Dissertation, Hamburg university, Germany. (2012).

[9] E. L. Saldin, E. A. Schneidmiller and M. V. Yurkov (2000), *The Physics of Free Electron Lasers.*, Springer-Verlag Berlin Heidelberg.

[10] Joseph W. Goodman (2007), Speckle Phenomena in Optics. *Theory and Applications.,* Ben Roberts & Company.